CASE 63

Steering System On-Center Robustness

Abstract: Traditionally, on-center steering response for a vehicle has been evaluated primarily through testing performed on actual prototype vehicles. A good on-center steering system is such that the driver can perceive small changes in road reaction forces through the steering wheel. This allows a driver to respond to slight changes in the vehicle heading. This is typically referred to as *on-center road feel*. A good on-center steering system will also have high overall stiffness, to achieve a narrow center and quick response.

The purpose of this study was to determine the steering system parameter values that optimize the robustness of vehicle on-center steering performance. A full vehicle ADAMS dynamic simulation model was used to generate all data required. The study employs the latest robust design methodology, incorporating the ideal function and Taguchi's dynamic signal-to-noise (SN) ratio.

1. Introduction

The goal of this project was to determine the vehicle steering and suspension system combination that optimizes the robustness of on-center steering performance. An ADAMS dynamic simulation computer model of a light truck vehicle was used to generate the data necessary for evaluation of the design. The model consisted of a detailed representation of the steering system combined with a full vehicle model. To establish the validity of the ADAMS model, the steering system and vehicle responses predicted were correlated with on-center road test data from a baseline vehicle prior to performing this study.

Many steering systems fail to achieve good on-center steering system performance, due partly to large amounts of lash and friction. A steering system with good road feel at high speeds must have maximum stiffness and minimum friction. These parameters are especially important in the on-center region, so that the driver can detect and respond to extremely small changes in road reaction forces resulting from road camber, bumps, wind, and so on, so as to maintain a constant heading.

There are limits as to what information from the road and vehicle the driver should be subjected to at the steering wheel. For higher-frequency noise, the steering system should function as a low-pass band filter that suppresses noise above 10 Hz from the road or vehicle but allows lower-frequency noise, below 3 Hz, through to the driver, so that the driver can respond appropriately and make corrections to his or her heading without having to rely solely on visual indicators, such as waiting for the vehicle to drift sufficiently far from the center of a traffic lane.

A steering system should also have linear on-center sensitivity, so that for small steering wheel angles, an increase in the steering wheel angle results in a proportional increase in the lateral acceleration experienced by the vehicle. The steering sensitivity level desired for a particular vehicle depends on the targeted image for that vehicle within the market.

Another important consideration in steering system on-center performance is the amount of dead

Taguchi's Quality Engineering Handbook. Genichi Taguchi, Subir Chowdhury and Yuin Wu

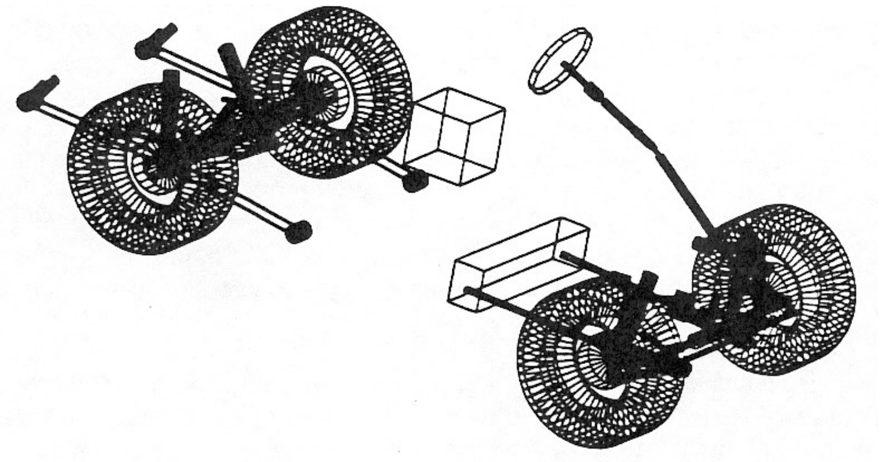

Figure 1
ADAMS full vehicle model

band in the system. This is a result of the hysteresis in the response of the vehicle to steering wheel inputs. Typically, smaller dead bands are preferred, but they cannot be eliminated entirely, due to a large contribution from the overall vehicle dynamics. The hysteresis is a function of the peak lateral acceleration, since larger accelerations will excite more nonlinear vehicle and tire dynamics.

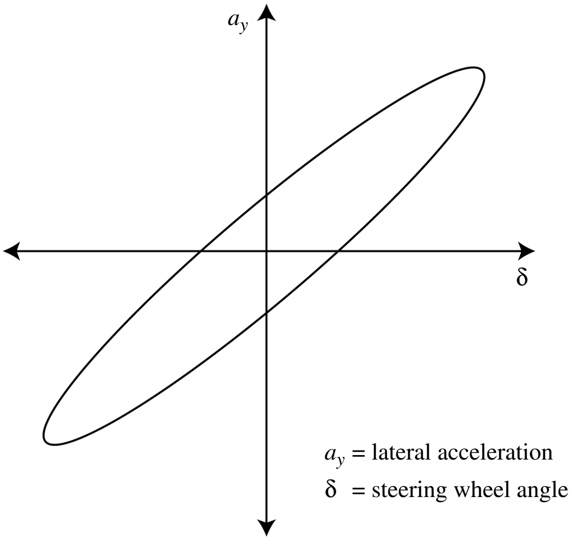

a_y = lateral acceleration
δ = steering wheel angle

Figure 2
Typical data for on-center a_y versus δ cross plot

2. Description of the Model

The steering system model, with over 90 degrees of freedom, is highly detailed in its description of individual steering system components. It was coupled with a full vehicle ADAMS model developed by Ford Light Truck Engineering (Figure 1).

Inputs to the steering system are at the steering wheel, and the outputs are reflected in the lateral acceleration response of the vehicle to the steering wheel input angle. For the on-center test simulated in this study, a sinusoidal steering wheel input at 0.2 Hz was imposed with a constant amplitude designed to generate an approximate 0.2-g peak lateral acceleration at a forward vehicle speed of 60 mph. A low level of lateral acceleration was chosen to reduce the nonlinear effects of vehicle dynamics on the on-center performance, so that the steering system performance could be isolated and evaluated.

Outputs from the simulation were characterized by plotting the vehicle lateral acceleration versus the steering wheel angle (Figure 2). The speed of the vehicle was varied, as in an ordinary on-center test, while the steering wheel angle amplitude was held

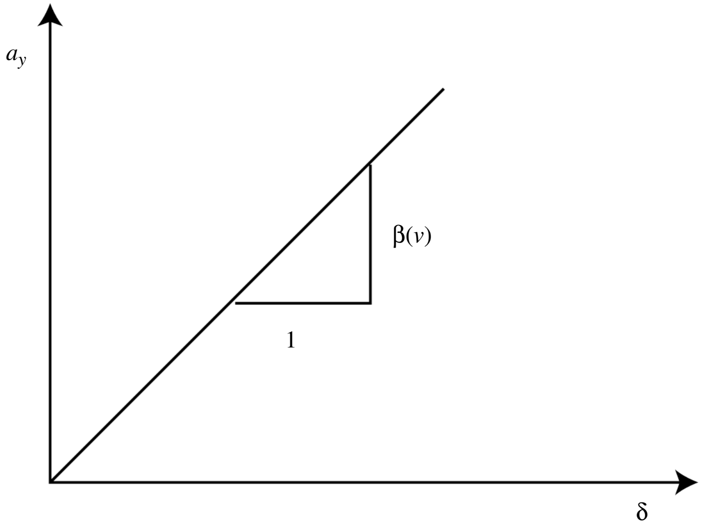

Figure 3
Ideal function for on-center steering

constant throughout the simulation. Results from actual vehicle on-center tests are typically characterized by the features defining the shape of the curve in cross plots of input and output variables. Among the significant indicators are the slope of the loop, which is a measure of hysteresis in vehicle-handling performance.

Steering sensitivity is a measure of the responsiveness of the vehicle to steering wheel inputs, usually tailored to fit a specific target value that depends on the vehicle image desired. As an example, sporty vehicles would typically be targeted to have a higher steering sensitivity than a family sedan would. Steering sensitivity is essentially a nominal-the-best target.

Hysteresis at low levels of peak lateral acceleration is an indicator of the lash and friction in the steering system, as well as the dynamic contribution due to the suspension and tires. At higher levels of vehicle lateral acceleration, hysteresis increases due to vehicle roll dynamics in the suspension and other nonlinearities in the tires and steering. Hysteresis can be thought of as a lag in the response of the vehicle to steering system inputs. Increased lag in the steering system response results in more steering dead band, which is undesirable. In this sense, hysteresis may be considered as a smaller-the-better target.

3. Ideal Function

Much discussion and effort went into defining the ideal function for the case study. After careful consideration of many possible alternatives, it was decided that the ideal function characterizing the steering system model on-center behavior would be best represented by an equation of the form

$$a_y = \beta(v)\delta$$

where a_y is the lateral acceleration of the vehicle (g), $\beta(v)$ the sensitivity coefficient as a function of vehicle speed (g/deg), (v is the vehicle speed in mph), and δ the steering wheel angle (deg). This formulation, shown in Figure 3, allowed for consideration of vehicles with both constant and varying understeer. The formulation also assumed that hysteresis is a condition to be minimized in the steering system. In fact, hysteresis was treated as part of the noise in formulating the system's SN ratio. Nonetheless, it was recognized that hysteresis is inherent in the vehicle dynamics and cannot be eliminated entirely from the steering system performance.

Selection of the ideal function was based on the assumption that the steering system open-loop function is as shown in Figure 3, where steering wheel angle (δ) is the driver input and lateral acceleration (a_y) of the vehicle is the output.

The ideal function selected for this study was derived from the results of an on-center steering test. The steering wheel angle versus lateral acceleration cross plot shown in Figure 2 is representative of a typical curve obtained from a vehicle on-center test. It can be seen that the ideal function shown in Figure 3 is a representation of the overall slope of the loop, but without hysteresis.

The response of the system in Figure 4 can be affected by environmental and other factors outside the direct control of the design engineer. Such factors are referred to as noise factors. Examples of noise factors are tire inflation pressure, tire wear, and weight distribution. It is necessary to design the system to achieve the most consistent input/output response regardless of the operating conditions experienced by the customer. Figure 5 shows the overall system diagram, indicating the noise factors and control factors considered in this study.

4. Noise Strategy

Several noise factors are shown in Figure 5. However, it is not necessary that all noise factors be included in the analysis. Typically, if a system is robust against one noise factor, it will be robust against other noise factors having a similar effect on the system. Therefore, the noise factor strategy involves selecting a subset of noise factors from all possible noise factors affecting the system. The noise factors selected should be those factors that tend to excite the greatest variation in the system response.

The steering system response to noise has two significant modes, one being the change in slope of the ideal function (sensitivity), the other a change in the size of the hysteresis loop. Therefore, it is necessary to group the noise factors into subsets, each of which excites one or the other mode of response to variations in noise levels. For example, some noise levels may expand the hysteresis loop with little or no effect on the steering sensitivity. These will be referred to as type P noise. Other noise factors may affect the slope of the loop, but not the width, thus affecting only steering sensitivity and not hysteresis, which will be referred to as Type Q noise. Any noise factors found to influence both modes simultaneously are not acceptable as part of the noise strategy, since these will impose interactions in the effects of noise on the system.

A study was conducted wherein each noise factor was varied individually between high and low levels using the vehicle steering system. Each noise factor was ranked according to its effect on the system response for both noise-induced response modes (i.e., hysteresis and/or sensitivity effects).

It was decided to select the two most significant noise factors affecting each of the two modes of noise-induced system response variability. Although column lash appeared second in significance in terms of the sensitivity variability, it also exhibited a strong interaction with the hysteresis mode. Thus, column lash was not a good candidate for the noise strategy, since it excited both noise modes simultaneously, which precluded separation of the effects of the two types of noise-induced modes on the system. Therefore, the noise strategy was as shown in Table 1, where the associated noise factor levels for each noise level (N_1 to N_4) are also indicated.

5. Case Study Results

The analysis was performed using an L_{27} array to accommodate three levels of each control factor and was conducted for three speeds: 45, 60, and 75 mph. Each ADAMS run generated response curves similar to those in Figure 2, where the lateral acceleration of the vehicle was plotted against steering wheel angle. From these curves, a least squares linear fit was made (passing through the origin), using points on both the top and bottom halves of the

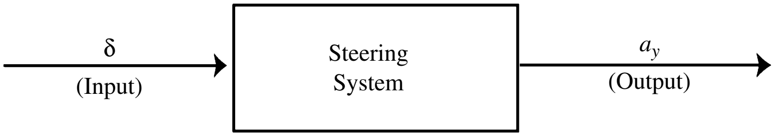

Figure 4
Steering system function

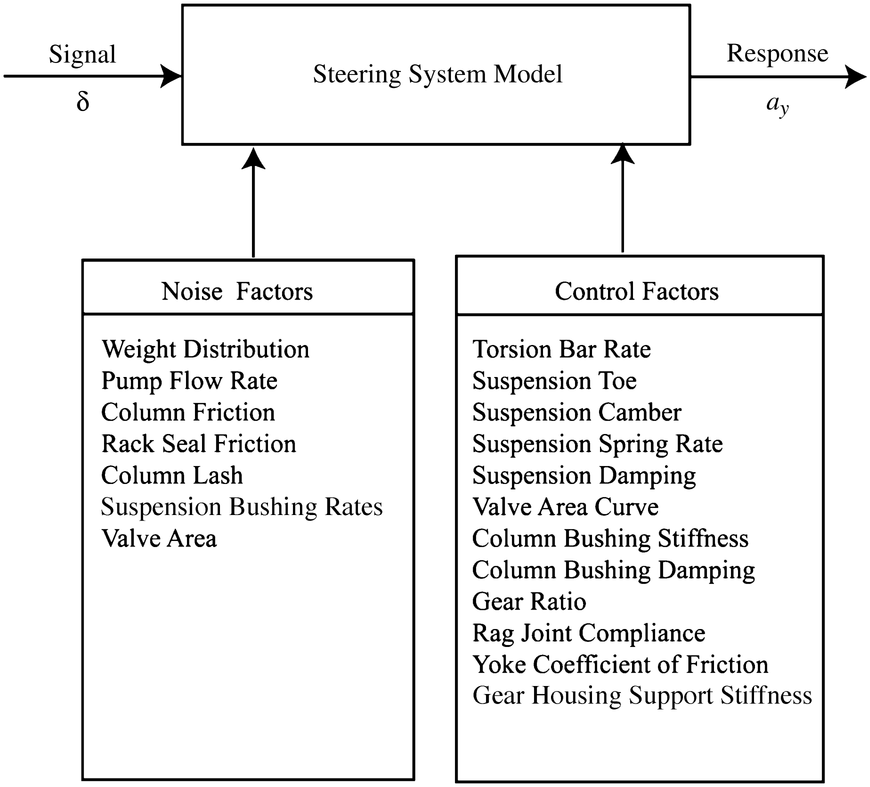

Figure 5
Engineering system for the steering system model

Table 1
Noise strategy

	Noise Level			
Noise Factor	**N_1 P_1, Q_1**	**N_2 P_1, Q_2**	**N_3 P_2, Q_1**	**N_4 P_2, Q_2**
Rack friction	Low	Low	High	High
Column friction	Low	Low	High	High
Weight distribution	High	Low	High	Low
Valve areas	High	Low	High	Low

loop. This line represents the ideal function of the steering system. The closer the actual data correspond with the straight-line approximation, the better the robustness of the system. Figure 6 illustrates the best-fit approach.

6. Analysis

For each run in the L_{27} array used in this experiment, an evaluation of the SN ratio can be made, using the relationship

$$\mathrm{SN} = 10 \log \left(\frac{\beta^2}{\sigma^2}\right)$$

where, SN is the signal-to-noise ratio (dB), β the sensitivity (g/deg), and σ^2 the variance (g^2). Although the SN ratio is a concept used extensively in control theory, it has application to general systems analysis as well. For the SN ratio to be maximized, the variance must be low, which indicates that the system response is consistent over a wide range of inputs and that its sensitivity to noise effects is small.

A robust system is one that results consistently in the corresponding ideal output signal response, as determined by the system ideal function (Figure 3), regardless of the noise factor levels in the surrounding environment. Keeping this definition in mind, it is apparent how the SN ratio can be used as an effective measure of system robustness.

In analyzing the SN data resulting from the simulations, it was decided first to perform separate robustness analysis for each of the three simulation velocities: in effect, with the assumption that the on-center robustness of the steering system is independent of vehicle speed. If this analysis were to produce varying results at different vehicle speeds, a more sophisticated approach to handling the data would be required to reconcile the results from varying speeds.

The SN ratio for each of the runs in the L_{27} array was computed over the signal levels (steering wheel angle inputs) and noise factor levels (N_1 to N_4) for each run. Next, an average was computed for each of the three levels for every control factor. A similar calculation was performed for the sensitivity (β) value.

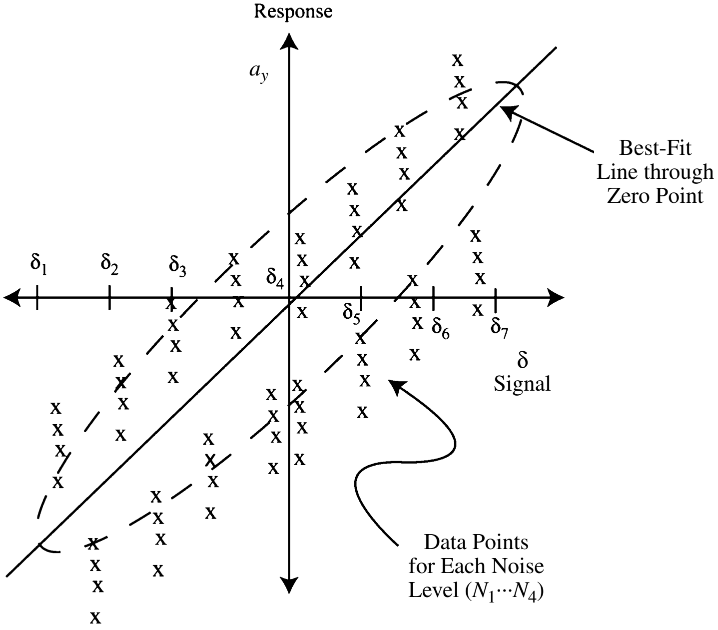

Figure 6
Best-fit approximation

With the average SN ratios, the optimum configuration was selected for maximizing the robustness of the system by choosing the level of each control factor with the highest SN ratio. An estimate of the overall system SN ratio was then obtained by summing the improvements due to each optimal control factor setting from the overall average of SN ratios for all 27 runs.

7. Simulation Results and Analysis of Data

A procedure for automating successive ADAMS simulation runs was developed and executed using a series of input data sets for each configuration (324 total) and command scripts to queue the analyses. Results were postprocessed automatically to obtain tabular data for the steering wheel angle versus vehicle lateral acceleration curve using seven steering wheel angle values, from −15 to +15° to define the upper and lower halves of the curve. The tabular data were then transferred into a spreadsheet that performed the curve fit (Figure 6) and least squares regression analysis, to compute the SN ratio and sensitivity values. As mentioned earlier, each of the three vehicle speeds was treated separately.

Results showed that the change in SN ratio from one run to the next were fairly consistent, regardless of vehicle speed. Also, a similar correlation was observed for the sensitivity, with the sensitivity increasing proportionally with vehicle speed. Thus, the signal quality (SN ratio) was independent of vehicle speed for the range of speed considered in this analysis, and the relative sensitivity was also unaffected by changes in vehicle speed. Therefore, results are presented and discussed only for the 60-mph vehicle speed simulations.

Table 2 shows the SN ratios and sensitivities computed for each of the 27 runs in the experiment for 60-mph vehicle speed. Using the data in the table, it is possible to calculate the SN ratio and sensitivity average for each of the three levels of control factors. Tables 3 and 4 show the average SN ratios and sensitivity values for the control factor levels at 60 mph. The average SN ratios for the torsion bar rate control factor levels at 60 mph, using the data in Table 1, were computed as follows.

Level 1:

$$\left(\frac{S}{N}\right)_{\text{av}} = \frac{1}{9} - 18.6 - 18.4 - 18.3 - 18.9 - 18.9 - 18.9 - 19.8 - 19.9 - 19.9) = -19.06$$

Level 2:

$$\left(\frac{S}{N}\right)_{\text{av}} = \frac{1}{9}(-20.0 - 20.0 - 20.2 - 18.4 - 18.4 - 18.2 - 18.5 - 18.7 - 18.6) = -19.02$$

Level 3:

$$\left(\frac{S}{N}\right)_{\text{av}} = \frac{1}{9}(-18.9 - 19.1 - 19.0 - 19.8 - 19.6 - 19.9 - 18.4 - 18.2 - 18.3) = -19.01$$

A chart comparing the effect on the SN ratios for the various control factor levels is presented in Figure 7 for the 60-mph simulations, and a similar plot for the sensitivity is shown in Figure 8.

From the individual control factor average SN ratio values shown in Figure 7 it is possible to predict the SN ratio for the optimum configuration, using the equation

$$\left(\frac{S}{N}\right)_{\text{opt}} = \left(\frac{S}{N}\right)_{\text{av}} + \sum_{n} \left[\left(\frac{S}{N}\right)_{n,\text{opt}} - \left(\frac{S}{N}\right)_{\text{av}}\right]$$

where

$\left(\frac{S}{N}\right)_{\text{opt}}$ = optimum configuration SN ratio

$\left(\frac{S}{N}\right)_{\text{av}}$ = average SN ratio for all runs in the L_{27} array

$\left(\frac{S}{N}\right)_{n,\text{opt}}$ = average SN ratio for the *n*th control factor at the optimum level

For example, the optimum configuration at 60 mph is given by selecting the following levels for each control factor, which represent the highest SN ratio values as shown in Table 3.

Optimum control factor levels at 60 mph:

$$A_3 \quad B_3 \quad C_1 \quad D_1 \quad E_2 \quad F_1 \quad G_3$$
$$H_3 \quad I_2 \quad J_3 \quad K_1 \quad L_3$$

Table 2
Summary of results for the L_{27} array at 60 mph

	Factor[a]													
Run	***A***	***B***	***C***	***D***	***E***	***F***	***G***	***H***	***I***	***J***	***K***	***L***	**SN**	**β**
1	1	1	1	1	1	1	1	1	1	1	1	1	−18.6	0.724
2	1	1	1	1	2	2	2	2	2	2	2	2	−18.4	0.730
3	1	1	1	1	3	3	3	3	3	3	3	3	−18.3	0.740
4	1	2	2	2	1	1	1	2	2	2	3	3	−18.9	0.749
5	1	2	2	2	2	2	2	2	3	3	1	1	−18.9	0.802
6	1	2	2	2	3	3	3	1	1	1	2	2	−18.9	0.755
7	1	3	3	3	1	1	1	3	3	3	2	2	−19.8	0.802
8	1	3	3	3	2	2	2	1	1	1	3	3	−19.9	0.754
9	1	3	3	3	3	3	3	2	2	2	1	1	−19.9	0.803
10	2	1	2	3	1	2	3	1	2	3	1	2	−20.0	0.669
11	2	1	2	3	2	3	1	2	3	1	2	3	−20.0	0.669
12	2	1	2	3	3	1	2	3	1	2	3	1	−20.2	0.729
13	2	2	3	1	1	2	3	2	3	1	3	1	−18.4	0.818
14	2	2	3	1	2	3	1	3	1	2	1	2	−18.4	0.775
15	2	2	3	1	3	1	2	1	2	3	2	3	−18.2	0.741
16	2	3	1	2	1	2	3	3	1	2	2	3	−18.5	0.826
17	2	3	1	2	2	3	1	1	2	3	3	1	−18.7	0.852
18	2	3	1	2	3	1	2	2	3	1	1	2	−18.6	0.830
19	3	1	3	2	1	3	2	1	3	2	1	3	−18.9	0.668
20	3	1	3	2	2	1	3	2	1	3	2	1	−19.1	0.730
21	3	1	3	2	3	2	1	3	2	1	3	2	−19.0	0.722
22	3	2	1	3	1	3	2	2	1	3	3	2	−19.8	0.785
23	3	2	1	3	2	1	3	3	2	1	1	3	−19.6	0.762
24	3	2	1	3	3	2	1	1	3	2	2	1	−19.9	0.791
25	3	3	2	1	1	3	2	3	2	1	2	1	−18.4	0.852
26	3	3	2	1	2	1	3	1	3	2	3	2	−18.2	0.808
27	3	3	2	1	3	2	1	2	1	3	1	3	−18.3	0.771

[a] *A*, torsion bar rate; *B*, gear ratio; *C*, valve curve; *D*, yoke friction; *E*, column bearing radial stiffness; *F*, column bearing radial damping; *G*, rag join torsional stiffness; *H*, gear housing support radial stiffness; *I*, suspension torsion bar rate; *J*, shock rate; *K*, toe alignment; *L*, camber alignment.

Table 3
SN ratios for control factor levels at 60 mph

	Factor											
Level	***A***	***B***	***C***	***D***	***E***	***F***	***G***	***H***	***I***	***J***	***K***	***L***
1	−19.06	−19.15	−18.93	−18.35	−19.03	−19.02	−19.08	−19.04	−19.07	−19.04	−19.02	−19.11
2	−19.02	−19.00	−19.09	−18.84	−19.03	−19.03	−19.03	−19.03	−19.01	−19.03	−19.03	−19.02
3	−19.01	−18.93	−19.07	−19.89	−19.03	−18.98	−19.02	−19.01	−19.02	−19.03	−19.03	−18.95
Delta	0.05	0.22	0.16	1.54	0.00	0.01	0.10	0.02	0.06	0.02	0.01	0.16

Table 4
Sensitivities for control factor levels at 60 mph

	Factor											
Level	***A***	***B***	***C***	***D***	***E***	***F***	***G***	***H***	***I***	***J***	***K***	***L***
1	0.762	0.709	0.782	0.773	0.766	0.764	0.762	0.751	0.761	0.765	0.756	0.789
2	0.768	0.775	0.756	0.771	0.765	0.765	0.766	0.765	0.764	0.764	0.766	0.764
3	0.765	0.811	0.757	0.752	0.765	0.767	0.768	0.779	0.770	0.766	0.773	0.742
Delta	0.006	0.102	0.026	0.021	0.001	0.003	0.006	0.028	0.009	0.002	0.017	0.047

The average SN ratio for all 27 runs at 60 mph can be computed by averaging the SN ratios computed for the three levels of any control factor in Table 3, since these values represent averages of nine runs each, so that

$$\left(\frac{S}{N}\right)_{\text{av}} = \frac{-19.06 - 19.02 - 19.01}{3} = -19.03$$

Thus, the optimum SN ratio at 60 mph is

$$\begin{aligned}\left(\frac{S}{N}\right)_{\text{opt}} &= -19.03 + (-19.01 + 19.03) \\ &\quad + (-18.93 + 19.03) + (-18.93 + 19.03) \\ &\quad + (-18.35 + 19.03) + (-19.03 + 19.03) \\ &\quad + (-19.02 + 19.03) + (-18.98 + 19.03) \\ &\quad + (-19.02 + 19.03) + (-19.01 + 19.03) \\ &\quad + (-19.02 + 19.03) + (-19.02 + 19.03) \\ &\quad + (-18.95 + 19.03) \\ &= -17.94\end{aligned}$$

The optimum control factor configuration at each vehicle speed was predicted. Similarly, predictions were also made for the worst-case configuration, having control factor-level settings corresponding to the lowest SN ratios as well as for the nominal configuration. The SN ratios predicted were verified by performing simulation at the control factor-level settings corresponding to the configuration predicted (optimum, nominal, and worst-case) and performing regression analysis to determine the actual SN ratio. Table 5 compares the results of the confirmation runs for all three cases: optimum, worst-case, and nominal. Values predicted were in good agreement with actual values, indicating that there are negligible interactions among the control factors.

Once the optimum control factor settings were determined to optimize system robustness, it was necessary to determine which control factors could be used to tune the system sensitivity to the target value desired. It can be seen in Figure 8 that the gear ratio has by far the greatest effect on the sensitivity, with several other parameters, such as camber, having appreciable effects as well. In using the gear ratio or camber as control factors to tune the steering system, there will be a slight effect on the steering system robustness. Camber changes will also affect tire wear characteristics, making it a poor choice for steering sensitivity adjustment. Among the control factors that had no appreciable effect on the steering system robustness (SN ratio) and that exhibited an effect on the sensitivity were the gear housing support radial stiffness and toe alignment angle.

Thus, the gear ratio, toe alignment, and gear housing support stiffness are good candidates as control factors available for tuning the system sensitivity. However, the gear ratio is probably the most practical, as changes to the gear housing support stiffness will also have an effect on the vehicle understeer characteristics. The toe alignment effect on steering sensitivity is in a rather narrow range, and there is evidence of toe alignment changes having an increasing effect on the steering system robustness at higher speeds, indicating that at very high speeds, toe effects may influence system robustness appreciably.

One other important observation from this study relates to the control factors that had no appreciable effect on the steering system robustness and sensitivity: including the column bearing radial

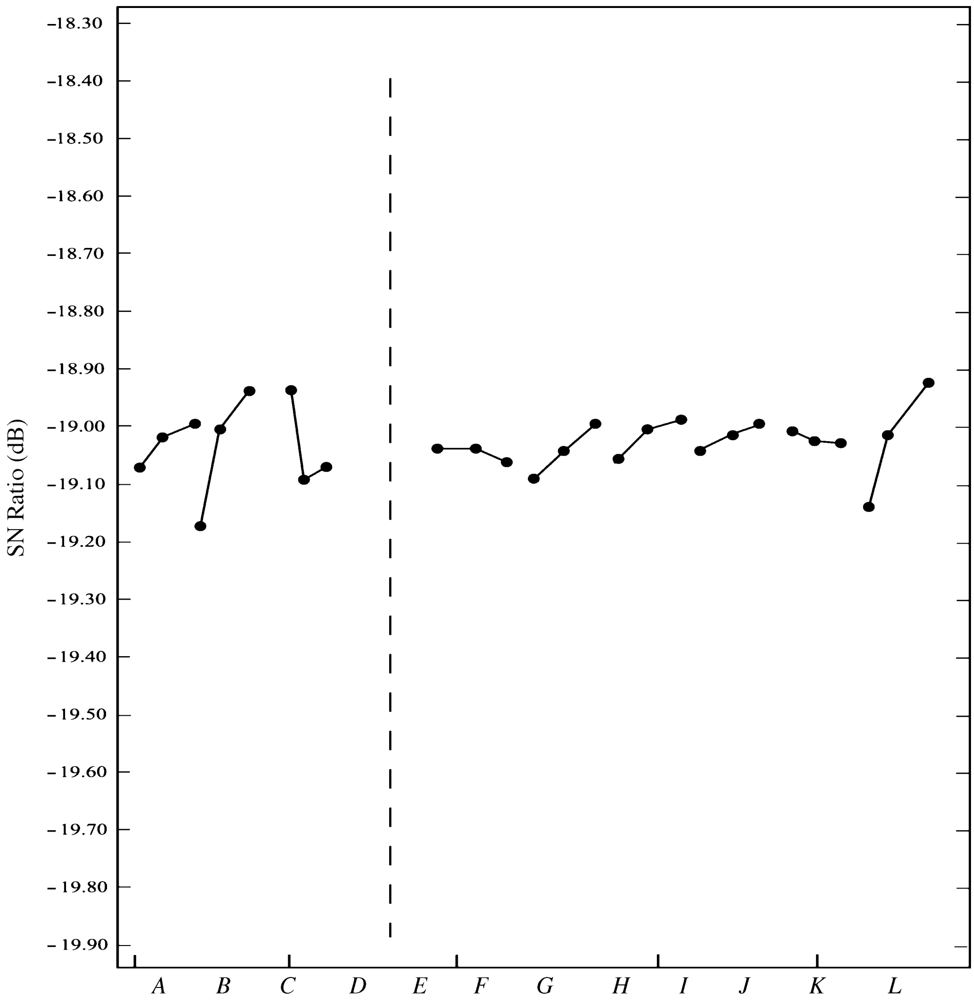

Figure 7
SN ratio comparison for control factor levels at 60 mph

stiffness, column bearing radial damping, and shock rate. These factors can be set to any level without affecting steering system robustness or sensitivity, and they can therefore be eliminated from consideration in any future on-center steering system robustness studies.

8. Conclusions

The close correlation between predicted and actual SN ratios and sensitivities for the optimum, nominal, and worst-case configurations demonstrate that the Taguchi robustness system analysis approach is accurate. Close correlation also indicates that there is little interaction between the control factors.

Important control factors for optimizing the steering system on-center robustness include the yoke friction, torsion bar rate, valve curve, gear ratio, rag joint torsional stiffness, camber angle, and suspension torsion bar rate. Other control factors, such as column bearing radial stiffness and damping, gear housing support radial stiffness, shock rate, and toe alignment angle had no effect on the

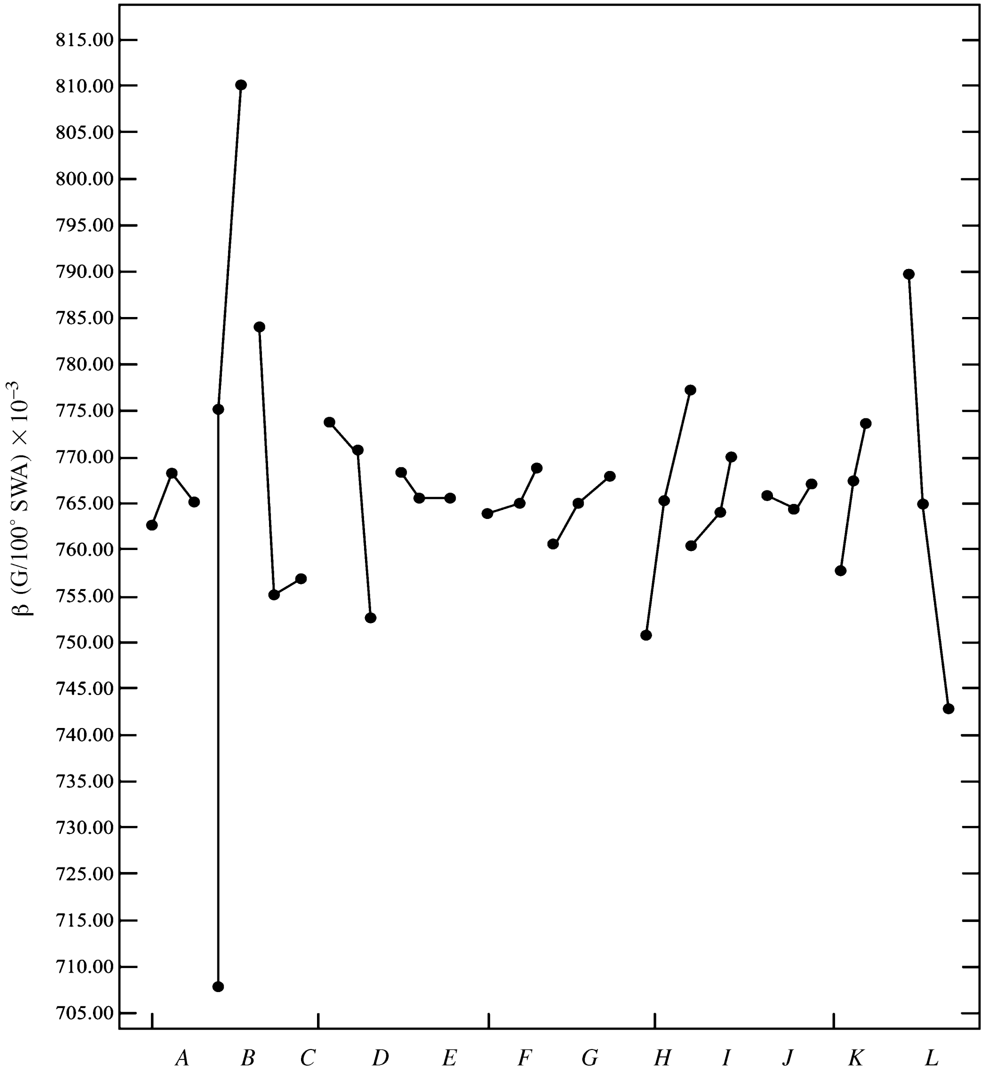

Figure 8
Sensitivity (β) comparison for control factor levels at 60 mph

SN ratio and can be set at any level desired without affecting steering system robustness. Future studies can narrow down control factors, eliminating those with little or no effect on signal quality in order to reduce the size of the problem.

In evaluating the optimum control factor levels, it is important to keep in mind other steering system considerations that may be affected by changes in the design. For example, the torsion bar rate increase will result in greater steering effort, which may be unacceptable. Also, yoke friction and rag joint stiffness changes may reduce the noise-handling characteristics of the steering system, requiring further design changes, such as incorporating a vibration damper into the steering system.

The SN ratio change from nominal to optimum is on the order of 1.6 dB for all speeds, which translates into an improvement of about 17%. The

Table 5
Predicted versus actual SN ratios (dB)

	45 mph		60 mph		75 mph	
Configuration	**Predicted**	**Actual**	**Predicted**	**Actual**	**Predicted**	**Actual**
Optimum	−17.75	−17.80	−17.94	−18.01	−17.85	−17.95
Nominal	−19.47	−19.41	−19.65	−19.58	−19.57	−19.52
Worst-Case	−19.94	−19.90	−20.33	−20.27	−20.31	−20.31

improvement in signal quality is especially apparent in Table 4, where the current nominal level is much closer to the worst-case configuration than to the optimum. Subjectively, a driver can sometimes perceive even a 0.25-dB improvement.

In general, control factors influence steering sensitivity and steering system signal quality (SN ratio) in the same way over the range of speed studied. Thus, future on-center steering system studies can be performed without the need to consider several speeds, thereby reducing overall simulation requirements.

Gear ratio and camber are the most important control factors in determining the sensitivity of the steering system, among those investigated in this analysis. The gear housing support stiffness is a good candidate for adjusting vehicle steering sensitivity within a limited range without affecting steering system on-center robustness. However, it may have an effect on understeer and other handling characteristics of the vehicle that must be considered.

Since friction plays such a dominant role in determining signal quality, it is important to study in further detail sources of friction in the rack, particularly the yoke, gear, and seal friction. Efforts are currently under way to study yoke and seal frictional effects, with the intent to incorporate more sophisticated gear friction models into the vehicle simulation model.

The main benefits of using the dynamic simulation techniques outlined in this study are reduced product development cost and time, achieved by a reduction in actual vehicle development test requirements. In addition, the development engineer can study many more possible design combinations than can be accomplished by exercising even the most ambitious vehicle development testing programs. Dynamic computer simulation techniques offer a much more versatile method by which to determine the best system configuration for product performance and quality.

Acknowledgments We would like to thank the following additional case study team members from the Ford Motor Company, Car Product Development, for their contributions to the project: Chris D. Clark, Paul Hurley, Phil Lenius, and Bernard Los. We would also like to thank Don Tandy and the people from the Vehicle Dynamics Section, Chassis Engineering, Light Truck Engineering, at Ford Motor Company for their work in developing the ADAMS vehicle model that made this case study possible. Finally, we would like to thank Genichi Taguchi and Shin Taguchi of the American Supplier Institute and John King and John Coleman at the Ford Design Institute for their guidance and assistance with this project.

This case study is contributed by V. G. Lenses and P. Jayakumar.